Kinetic and Mechanical Basis of Rolling through an Integrin and Novel Ca^{2+}-Dependent Rolling and Mg^{2+}-Dependent Firm Adhesion Modalities for the $\alpha4\beta7$−MAdCAM-1 Interaction†

Maarten de Château,‡ Shuqi Chen, Azucena Salas, and Timothy A. Springer*

The Center for Blood Research, Department of Pathology, Harvard Medical School, 200 Longwood Avenue, Boston, Massachusetts 02115

Received July 31, 2001; Revised Manuscript Received September 12, 2001

ABSTRACT: We studied interactions in shear flow of cells bearing integrins $\alpha4\beta1$ or $\alpha4\beta7$ with VCAM-1 and MAdCAM-1 substrates in different divalent cations. Interestingly, Ca^{2+} was essential for tethering in flow and rolling interactions through both α4 integrins. Mg^{2+} promoted firm adhesion of $\alpha4\beta7$-expressing cells on MAdCAM-1 but with much lower tethering efficiency in shear flow. The $k_{off}°$ of 1.28 s^{-1} and resistance of the receptor−ligand bond to force (estimated as a bond interaction distance or σ) for transient tethers on MAdCAM-1 were similar to values for E- and P-selectins. By contrast to results in Ca^{2+} or Ca^{2+} + Mg^{2+}, in Mg^{2+} the $\alpha4\beta7$−MAdCAM-1 $k_{off}°$ decreased 20-fold to 0.046 s^{-1}, and the bond was weaker, providing an explanation for the finding of firm adhesion under these conditions. Shear enhanced tethering to MAdCAM-1, thereby contributing to the stability of rolling. Comparisons to selectins demonstrate that the kinetic and mechanical properties of the $\alpha4\beta7$ integrin are well suited to its intermediate position in adhesion cascades, in which it bridges rapid rolling through selectins to firm adhesion through $\beta2$ integrins.

Leukocyte recruitment in the vasculature at sites of inflammation and lymphocyte homing to lymphoid organs require multiple adhesive and signaling interactions. The adhesive interactions involve functionally specialized macromolecules on the surfaces of leukocytes and endothelial cells, including selectins, cell adhesion molecules (CAMs)[1] of the immunoglobulin superfamily (IgSF), and integrins. These molecules mediate the multiple steps that are required for leukocytes in the bloodstream to reach their specific tissue destination, including initial tethering to endothelial ligands, rolling, firm adhesion, and transmigration through the vessel wall (*1*, *2*). Although essentially all integrins mediate firm adhesion, a small subset of integrins can also mediate rolling: $\alpha4\beta1$, $\alpha4\beta7$, and $\alpha6\beta4$ (*3*−*5*) and, in special circumstances, $\alpha L\beta2$ (*6*, *7*).

The preferred endothelial cell ligands for $\alpha4\beta1$ and $\alpha4\beta7$ are vascular cell adhesion molecule-1 (VCAM-1) and mucosal addressin cell adhesion molecule-1 (MAdCAM-1), respectively (*8*, *9*). The major form of VCAM-1 has seven extracellular, Ig-like domains and is upregulated on endothelia in response to inflammatory stimuli (*10*). MAdCAM-1 is expressed on endothelia in mucosal tissue and Peyer's patches and helps to target lymphocytes bearing $\alpha4\beta7$ to these sites (*9*, *11*). MAdCAM-1 has two NH_2-terminal Ig domains and a more C-terminal, membrane-proximal, mucin-like region (*9*, *12*).

Divalent cations are essential for ligand binding by integrins. Divalent cations may influence ligand binding by stabilizing particular integrin conformations, by forming part of the ligand binding site, or may act through both of these mechanisms (*13*). Under static conditions, many integrin−ligand interactions show binding in the presence of Mg^{2+}, even stronger binding in Mn^{2+}, and no or little binding in Ca^{2+} (*14*−*22*). Some interactions, like that of $\alpha2\beta1$ with collagen, LFA-1 with ICAM-1, $\alpha V\beta3$ with fibrinogen, and $\alpha5\beta1$ with fibronectin, show antagonism between Mg^{2+} and Ca^{2+}; increased concentrations of Ca^{2+} inhibit Mg^{2+}-dependent binding (*21*−*24*). By contrast, Ca^{2+} can support ligand binding by a minority of integrins, including the α4 integrins. Ca^{2+} supports binding by platelet integrin $\alpha IIb\beta3$ to fibrinogen (*24*) and $\alpha4\beta1$ binding to VCAM-1 but not $\alpha4\beta1$ binding to fibronectin (*25*). $\alpha4\beta7$ binding to MAdCAM-1 under static conditions was shown to be most efficient in Mn^{2+}, less so in Mg^{2+}, and lower but still significant in Ca^{2+} (*26*). Addition of Mn^{2+} had no effect on the efficiency of tethering of $\alpha4\beta1$ to VCAM-1 under flow but did result in conversion of rolling into firm adhesion (*27*). Mn^{2+} also stimulated firm adhesion of lymph node cells rolling on MAdCAM-1 (*4*).

Insights into the molecular properties that underlie rolling have emerged recently for selectins. Rolling cells move with a jerky, stepwise motion. The steps are accurately modeled as breakages of bond clusters (*28*). Breakage of individual

† This work was supported by NIH Grant HL48675.

* To whom correspondence should be addressed. Tel: (617) 278-3200. Fax: (617) 278-3232. E-mail: springeroffice@cbr.med.harvard.edu.

‡ Present address: Department of Genetics and Pathology, Rudbeck Laboratory, Uppsala University, S-751 85 Uppsala, Sweden.

[1] Abbreviations: BSA, bovine serum albumin; CAMs, cell adhesion molecules; EGTA, ethylene glycol bis(β-aminoethyl ether)-*N*,*N*,*N*′,*N*′-tetraacetic acid; LFA-1, lymphocyte fusion-associated antigen-1; mAb, monoclonal antibody; MAdCAM-1, mucosal adressin cell adhesion molecule-1; PBS, phosphate-buffered saline; VCAM-1, vascular cell adhesion molecule-1.

10.1021/bi011582f CCC: $20.00
Published on Web 10/26/2001

bonds can be visualized with transiently tethered cells (*3*). Transient tethers are seen when the substrate density is lower than that required to support rolling. Under these conditions, leukocytes moving at the hydrodynamic flow velocity will momentarily arrest on the substrate and then detach and resume movement at the hydrodynamic velocity. Transient tethers have first-order dissociation kinetics and other characteristics that are suggestive of single receptor−ligand bonds (*3*, *29*). Selectin−ligand off-rates are fast, as was hypothesized for receptors that support rolling (*30*).

The k_{off} of a receptor−ligand bond is a function of the applied force. The force on a receptor−ligand bond between a cell in shear flow and the substrate is related to the force on the cell, which is proportional to flow rate. Previous measurements have shown that k_{off} increases with force and that the relationship between k_{off} and force is approximately exponential (*3*, *29*, *31*−*35*). The amount by which force increases k_{off} differs for different receptor−ligand bonds and is termed the reactive compliance or mechanical property of the bond. Bonds that support rolling should be relatively force-resistant, i.e., mechanically strong. By contrast, an antibody−antigen bond has been shown to be less force resistant; in other words, it exhibited a greater increase in k_{off} at a given force than selectin bonds (*33*). Numerous relationships have been proposed between force and k_{off} (*36*−*39*). A recent comparison between these relationships for the P-selectin receptor−ligand bond (*40*) showed the best fit to the Bell model (*37*). In this model, bond dissociation increases exponentially with force, and the fit to the data yields the exponential constant known as σ, which is in units of length (*3*, *29*, *31*−*35*). The constant σ is known as the bond interaction distance or mechanical bond length and reflects the separation distance between the receptor and ligand over which bond strength weakens and k_{off} increases. In practice, factors other than separation, including the deformability of the domains bearing the receptor and ligand binding sites and extensibility of other domains in the receptor and ligand, are incorporated in the constant σ (*29*). Therefore, σ should not be interpreted literally as implying a bond dimension but is very useful in practice for summarizing in a single constant the mechanical properties of bonds; the smaller the σ, the less force increases k_{off}, i.e., the stronger the bond. The mechanical properties of integrin receptor−ligand bonds have not previously been measured and are of considerable interest for the comparison of selectin-mediated to integrin-mediated rolling.

Recently, it has been appreciated that, in addition to rapid on- and off-rates and mechanical strength, another property is important to stabilize rolling over the wide range of hydrodynamic forces that act on leukocytes in vivo. As hydrodynamic force on the cell increases, the increased rate of bond breakage is balanced by enhancement by shear of the rate of bond formation for E-selectin and L-selectin (*28*). It is of interest to determine whether integrins also exhibit shear-enhanced bond formation.

The α4 integrins can mediate both rolling and firm adhesion. This puts α4 integrins in a unique bridging position between rapid rolling through selectins and firm adhesion through β2 integrins (*41*−*44*). Because of this, and the interest in comparisons to selectins, we have measured for the integrin α4β7 the molecular parameters important for rolling. Previously, it had been known that both Ca^{2+} and Mg^{2+} could support adhesion through α4 integrins to CAMs in static assays (*25*, *26*), but no functional differences in Ca^{2+} and Mg^{2+} had been noted. Here, we find that Ca^{2+} supports rolling adhesion and Mg^{2+} supports firm adhesion through α4β7. The correlation with $k_{off}°$ and σ values in Ca^{2+} and Mg^{2+} provides new insights into rolling and firm adhesion modalities of α4 integrins.

EXPERIMENTAL PROCEDURES

Materials

Cells. RPMI 8866, a human B cell line (*45*), and KA4, a K562 erythroleukemia cell line stably transfected with the human integrin α4 chain (*46*), were maintained in RPMI 1640 medium with 10% fetal calf serum and gentamycin (10 μg/mL). RPMI 8866 cells were split at least 3-fold every 2−3 days with fresh medium and were maintained at lower cell densities at which they grew as single cells. Higher cell densities at which they grew in clumps were associated with firm rather than rolling adhesion on MAdCAM-1. Fresh aliquots of viably frozen cells were thawed every 2 months, because long periods of cell culture were also associated with cell clumping and firm adhesion. 293T cells were stably cotransfected with full-length human MAdCAM-1 cDNA in pcDNA3 (Invitrogen, Carlsbad, CA) and a puromycin resistance gene in pEFpuro by calcium phosphate precipitation (*47*). Clones growing in 2−4 μg/mL puromycin were picked and screened for MAdCAM-1 expression by immunofluorescence flow cytometry using MAdCAM-1 mAb 10G3 (*48*). Transfectants were maintained in DMEM with 4 μg/mL puromycin. To ensure firm anchoring, monolayers of transfected 293T cells were grown on polystyrene tissue culture dishes coated with poly-L-lysine hydrobromide (Sigma Chemical Co., St. Louis, MO) at 100 μg/mL in water on polystyrene tissue culture dishes for 5 min. The dishes were rinsed with water and dried for 2 h before addition of cells and medium. The cells were allowed to adhere and grow on the poly-L-lysine coated plates for at least 2 days before the flow chamber was assembled on top of the monolayer prior to experimentation.

Proteins. Recombinant soluble VCAM-1 (rsVCAM-1) containing seven Ig domains was a kind gift from Roy Lobb, Biogen Inc., Cambridge, MA, and was previously described (*49*). MAdCAM-1−Ig fusion protein was a kind gift of Michael J. Briskin, Leukosite Inc., Cambridge, MA, and has been described (*26*). Briefly, the extracellular domain of human MAdCAM-1 was fused to the constant region of human IgG1, expressed in NSO cell lines, and purified from culture supernatants by protein A affinity chromatography. mAbs HP2/1 (anti-α4), Dreg56 (anti-L-selectin), 13 (anti-β1), Hae-2a (anti-VCAM-1), and Act-1 (anti-α4β7) were from the fifth International Leukocyte Workshop (*50*), and the 10G3 mAb to MAdCAM-1 was from Michael J. Briskin (*48*).

Methods

Flow Cytometry. Immunofluorescence flow cytometry was as described (*51*).

Flow Chamber Assay. A polystyrene Petri dish was coated with a 5 mm diameter, 20 μL spot of purified protein (at 0.3−10 μg/mL as indicated) in PBS (pH 9.0) and 5 μg/mL

BSA for 1 h at 37 °C, followed by 20 mg/mL BSA in PBS for 1 h at 37 °C to block nonspecific binding sites. The supplementation with 5 μg/mL BSA was included with all MAdCAM-1 concentrations and prevented nonuniform coating of the substrate at low MAdCAM-1 densities. The dish was assembled as the lower wall of a parallel plate flow chamber and mounted on the stage of an inverted phase contrast microscope (*30*).

Protein site density was determined as described (*52*) as the number of ^{125}I-labeled mouse anti-MAdCAM-1 mAb 10G3 (*48*) and anti-VCAM-1 mAb Hae-2a (*53*) antibodies bound per μm^2, assuming a 1:1 stoichiometry. Site densities were linearly related to coating concentration in the range 0.3−10 μg/mL and were 50 sites/μm^2 per μg/mL for MAdCAM-1 and 20 sites/μm^2 per μg/mL for VCAM-1.

Cells were washed three times in Ca^{2+}- and Mg^{2+}-free Hank's balanced salt solution (HBSS)/10 mM Hepes (pH 7.4)/10 mM EDTA by centrifugation at 1200 rpm for 5 min. Cells were then resuspended at a concentration of 10^6/mL in Ca^{2+}- and Mg^{2+}-free HBSS/10 mM Hepes (pH 7.4) substituted with cations and EGTA at indicated concentrations. Using 1 mM $MgCl_2$ gave the same results as using 1.5 mM $MgCl_2$ with 0.5 mM EGTA. For experiments on monolayers of transfected cells, BSA (0.5 mg/mL) was added to the medium to minimize nonspecific interactions. Cells were perfused into the flow chamber at varying flow rates using a syringe pump. Microscopic images of cells were videotaped for later analysis.

Analysis of Flow Chamber Data. Data were analyzed with the help of a computerized imaging system consisting of a Pentium computer with MVC150/40-VL boards (Imaging Technology, Bedford, MA) and software developed by us (*28*).

Stable tethers were defined as cells rolling or firmly adhering for at least 3 s on the substrate. Only tethers formed in the field of view were counted. Tethering was determined by counting the number of cells that tethered during the first 40 s of continuous shear flow.

Detachment assays were performed on cells after they had tethered at low shear flow (0.4 dyn/cm^2) for 30 s. The shear flow was then increased every 10 s and the number of remaining cells counted at the end of each shear period. Rolling velocity determinations were performed as for detachment assays. Rolling cells were operationally defined as adherent cells that moved at ≥1.5 μm/s. The cutoff of 1.5 μm/s corresponds to a movement of less than one cell diameter during the meaurement period of 5 s. We used this cutoff because even firmly adherent cells may demonstrate extension of tethers as flow velocity is increased, with a creep of the cell body downstream in the absence of true rolling.

For transient tethers, MAdCAM-1 was diluted to 0.3−1.0 μg/mL in PBS. At least 30−40 transient tethering events were collected for each experimental group, and the lifetime of each tether was measured. The natural log of the number of cells that remained bound as a function of time after initiation of tethering was plotted. Data were plotted for the time period during which the percentage of transiently tethered cells dropped from 100% to 10%. These data showed a good fit to a straight line, demonstrating first-order dissociation kinetics. Therefore, k_{off} was determined as the slope of this line, −d(ln bound cells)/dt. The hydrodynamic force (F_s) on a tethered cell and the force on the tether bond were calculated as described previously (*3*). The lever arm acting on a tether was measured as described for P-selectin tethers (*29*) by reversing the direction of flow during transient tethering and measuring cell displacement. The lever arm = $^1/_2$ tethered cell displacement during flow reversal.

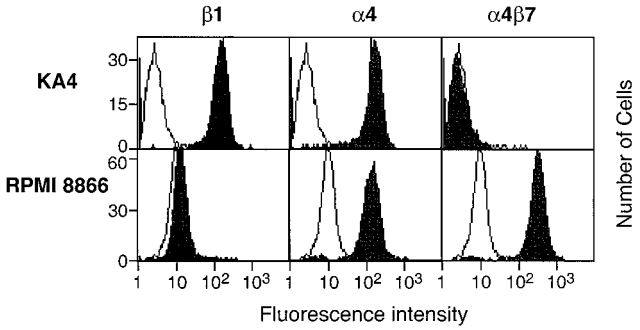

FIGURE 1: Immunofluorescence flow cytometry measurement of α4 integrins on the surface of RPMI 8866 and KA4 cells. Cells were incubated with a nonspecific mouse IgG1 (clear peak) or mAb 13 to the β1 subunit, mAb HP2/1 to the α4 subunit, or mAb Act-1 to the α4β7 complex (shaded peaks). Binding of primary antibody was detected with secondary antibody conjugated to FITC.

RESULTS

Tethering to MAdCAM-1 and VCAM-1 under Flow Conditions Depends on Calcium but Not Magnesium. To examine α4 integrin-mediated rolling on purified recombinant MAdCAM-1 and VCAM-1, cell lines selectively expressing α4β7 and α4β1 were chosen (Figure 1). The human B cell line RPMI 8866 (*45*) expresses α4 and β7 and little or no β1. The erythroleukemia cell line K562 stably transfected with α4, named KA4 (*46*), expresses α4 and β1 and little or no β7.

Initial experiments examined the specificity, divalent cation requirements, and shear profile of tethering to MAdCAM-1 and VCAM-1 (Figure 2). Stable tethering, defined as binding of cells in flow to substrates that was followed by rolling or firm adhesion that lasted for ≥3 s, was observed for RPM1 8866 cells on purified MAdCAM-1 substrates or 293T cells monolayers expressing MAdCAM-1 and for KA4 cells on purified VCAM-1. No stable tethers (<1% of control) were seen when no divalent cation was added to the buffer or when the buffer was supplemented with 10 mM EDTA (Figure 2A and data not shown). Stable tethering efficiency on MAdCAM-1 was highest at low wall shear stresses (Figure 2A,B) and was seen up to 2 dyn/cm^2 at 250 sites/μm^2 (Figure 2A). Tethering to MAdCAM-1 was highly specific since it was completely abolished by pretreatment of cells with mAb HP2/1 to α4 or mAb Act-1 to α4β7. No inhibition was seen if the cells were pretreated with control myeloma IgG1. The L-selectin mAb Dreg56, and fucoidin, each of which inhibit L-selectin function, had no effect on tethering to MAdCAM-1, either separately or together (Figure 2A). Therefore, indirect, L-selectin-dependent tethers of cells in flow to adherent cells (*54*) did not contribute to accumulation on MAdCAM-1. Furthermore, this confirmed that the mucin-like domain of the recombinant MAdCAM-1 did not bind L-selectin, as previously reported (*12*).

Different divalent cations were compared for support of tethering through α4β7. Tethering to MAdCAM-1, either

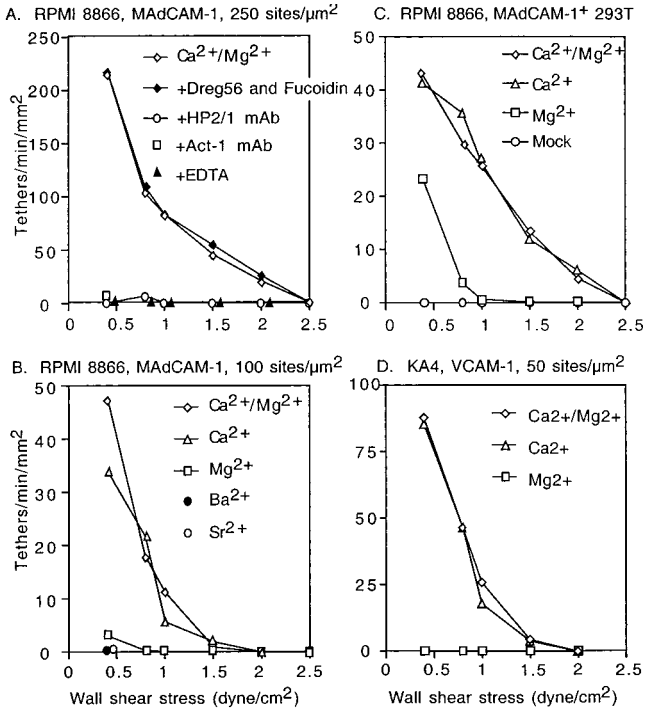

FIGURE 2: Ca^{2+} is sufficient to support leukocyte tethering through α4 integrins on MAdCAM-1 and VCAM-1. (A) Tethers of RPMI 8866 cells to purified MAdCAM-1 at 250 sites/μm^2. (B) Tethers of RPMI 8866 cells to MAdCAM-1 at 100 sites/μm^2. (C) Tethers to monolayers of 293T cells transiently transfected with MAdCAM-1 cDNA or vector alone (mock). (D) Tethers of KA4 cells to purified VCAM-1 at 50 sites/μm^2. The number of stably tethered cells that accumulated per 10× field (1.1 × 0.8 mm) was measured during 45 s on the indicated substrates as a function of wall shear stress. Stable tether interactions were defined as initial interactions between a cell at the hydrodynamic velocity and the substrate that were followed by at least 3 s of rolling or firm adhesion. Cells were washed three times in EDTA buffer and then suspended for flow assays in Ca^{2+}- and Mg^{2+}-free HBSS and 10 mM Hepes, pH 7.4, supplemented with either 1 mM $CaCl_2$, 1 mM $MgCl_2$, both cation salts at 1 mM each, or 1 mM $BaCl_2$ or $SrCl_2$. Fucoidin was at 10 μg/mL and antibodies were at 10 μg/mL.

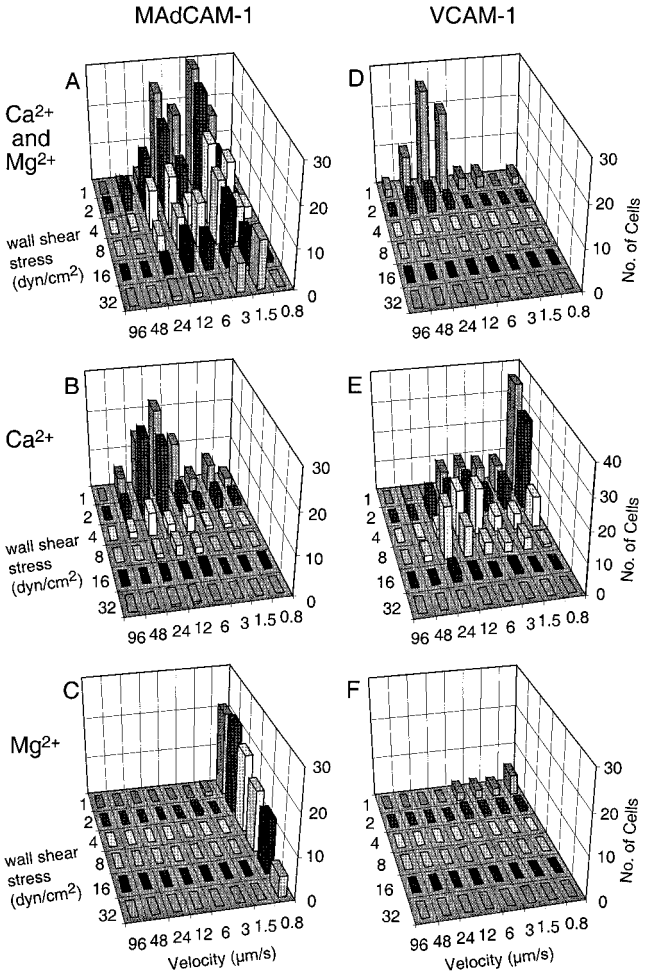

FIGURE 3: Rolling velocity distribution as a function of divalent cations and wall shear stress. RPMI 8866 cells were allowed to accumulate on MAdCAM-1 substrates (A−C), or KA4 cells were allowed to accumulate on VCAM-1 substrates (D−F) at 0.4 dyn/cm^2 for 30 s. Shear stress was then increased for 10 s durations to 1 dyn/cm^2 and in 2-fold increments of shear stress for 10 s durations thereafter. Rolling velocities were based on the distance rolled from 4 to 8 s of each shear interval. The rolling velocity of individual cells was calculated, and the number of cells within a given velocity range was counted to give the population distribution. Velocity intervals shown in the figure are 0−0.8, 0.8−1.5, 1.5−3, 3−6, 6−12, 12−24, 24−48, and 48−96 μm/s. Buffers contained in (A) and (D) were 1 mM $CaCl_2$ and 1 mM $MgCl_2$, in (B) and (E) 1 mM $CaCl_2$, and in (C) and (F) 1 mM $MgCl_2$.

as purified protein or as expressed on a monolayer of transfected 293T cells, was similarly efficient in buffer containing Ca^{2+} alone (1 mM) and in buffer containing both Ca^{2+} and Mg^{2+} (1 mM each) (Figure 2B,C). Surprisingly, there was much less or almost no tethering in the presence of Mg^{2+} alone (Figure 2B,C). The Ca^{2+} requirement is very stringent, because 1 or 5 mM concentrations of the chemically related divalent cations Sr^{2+} and Ba^{2+} did not support tethering to MAdCAM-1 (Figure 2B). Dependence on divalent cations was also tested for tethering of α4β1-expressing KA4 cells to VCAM-1 coated on plastic. Tethering in Ca^{2+} + Mg^{2+} was similar to that in Ca^{2+} alone, and there was no tethering in Mg^{2+} (Figure 2D). Thus, tethering of α4β1 to VCAM-1 is dependent on Ca^{2+}, just as found for α4β7 tethering to MAdCAM-1.

Ca^{2+} and Mg^{2+} Regulate Rolling Velocity, and Rolling As Opposed to Firm Adhesion, on MAdCAM-1 and VCAM-1. In the presence of different divalent cations, RPMI 8866 cells and KA4 cells were allowed to accumulate for 30 s at 0.4 dyn/cm^2 on MAdCAM-1 and VCAM-1 substrates, respectively. The wall shear stress was then increased to 1 dyn/cm^2, and in 2-fold increments thereafter, for 10 s each. The distribution of rolling velocities was determined for the population of adherent cells at each wall shear stress (Figure 3). The α4β7-dependent interaction of RPMI 8866 cells with MAdCAM-1 showed distinct adhesive modalities in Ca^{2+} and Mg^{2+} (Figure 3B,C). In Ca^{2+} alone essentially all adherent cells rolled (Figure 3B), whereas in Mg^{2+} alone all adherent cells were firmly adherent (Figure 3C). The cells firmly adherent to MAdCAM-1 in Mg^{2+} were more strongly adherent to the substrate than the rollingly adherent cells in Ca^{2+}; in Mg^{2+} half of the cells remained adherent up to 16 dyn/cm^2 (Figure 3C) whereas in Ca^{2+} less than half the cells remained adherent at 4 dyn/cm^2 (Figure 3B). In Ca^{2+} + Mg^{2+} (Figure 3A), a biphasic distribution of rolling velocities was seen; one phase represented slowly rolling cells, and the other phase represented cells that rolled more rapidly but more slowly than in Ca^{2+} alone (compare panels A and B of Figure 3). The resistance to detachment by shear seen in Ca^{2+} and Mg^{2+} (Figure 3A) was similar to that seen in Mg^{2+} alone (Figure 3C).

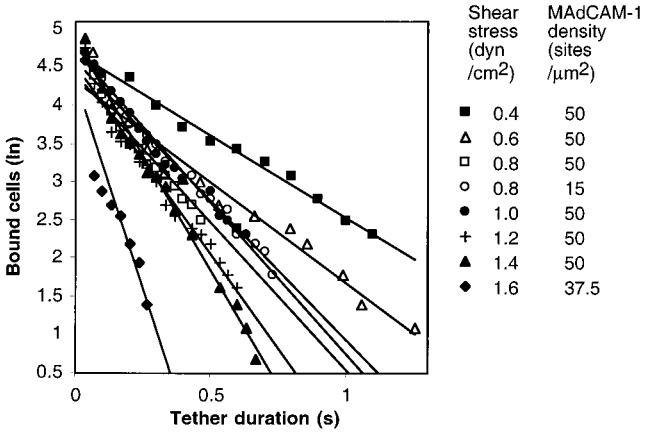

FIGURE 4: Kinetics of dissociation of transiently tethered cells. The duration was measured of transient tethers of RPMI 8866 cells on MAdCAM-1 substrates at the indicated density and wall shear stress. There was no significant difference in off-rates at different densities; representative results are shown at 0.8 dyn/cm^2 at 15 and 50 sites/μm^2. The natural logarithm of the number of cells that remain tethered is plotted as a function of time after initiation of the tether. Data are for the first ≥90% of the cells to dissociate (the time period during which bound cells declined from 100% to 10%).

The $\alpha4\beta1$ interaction with VCAM-1 was similar, in that Ca^{2+} was sufficient to support tethering and rolling adhesion (Figure 3D,E). However, the effects of Mg^{2+} differed. Fewer cells accumulated at 0.4 dyn/cm^2 on VCAM-1 than MAdCAM-1 in Mg^{2+} (panel F compared to panel C in Figure 3). Furthermore, in the presence of Ca^{2+} and Mg^{2+} (Figure 3D) compared to Ca^{2+} alone (Figure 3E), cells rolled faster and were less shear resistant.

Kinetic and Mechanical Properties of the α4β7−MAdCAM-1 Tether Bond. To understand the biophysical basis for rolling through an integrin and the novel and dramatic effects of Ca^{2+} and Mg^{2+} on rolling through $\alpha4\beta7$, we characterized the kinetics of transient tethers. At MAdCAM-1 densities ≤50 sites/μm^2, rolling did not occur, and cells in hydrodynamic flow were observed to transiently tether to the substrate and then resume movement at the hydrodynamic velocity. To examine the kinetics of cellular dissociation, the duration of the tethers was plotted (Figure 4). A log plot of the number of tethers remaining with time showed that, at least for the first 90% of cells to dissociate from the substrate, the kinetics followed a straight line (Figure 4). Therefore, the transient tethers demonstrated first-order dissociation kinetics consistent with dissociation of single receptor−ligand bonds as observed with selectins (*3*, *29*). Furthermore, at different densities of MAdCAM-1, tether dissociation kinetics did not vary, again consistent with single receptor−ligand bonds (Figures 4 and 5). As wall shear stress increased, k_{off} increased, as shown by the steeper slopes of semilog plots of tether duration (Figure 4).

We examined the mechanical stability of the $\alpha4\beta7$−MAdCAM-1 tether bond, i.e., the effect on k_{off} of force on the bond (F_b). For this, it was necessary to determine the relationship between the hydrodynamic force on a tethered cell and the force on the tether bond, which in turn requires measurement of the cell diameter and lever arm (Figure 5 inset). The lever arm was determined by measuring the distance that transiently tethered cells moved during flow reversal (*29*) (Figure 5 inset). The lever arm of RPMI 8866 cells on MAdCAM-1 was 4.6 ± 0.9 μm, and the RPMI 8866 cell diameter was 9.6 ± 1.1 μm (mean ± SD).

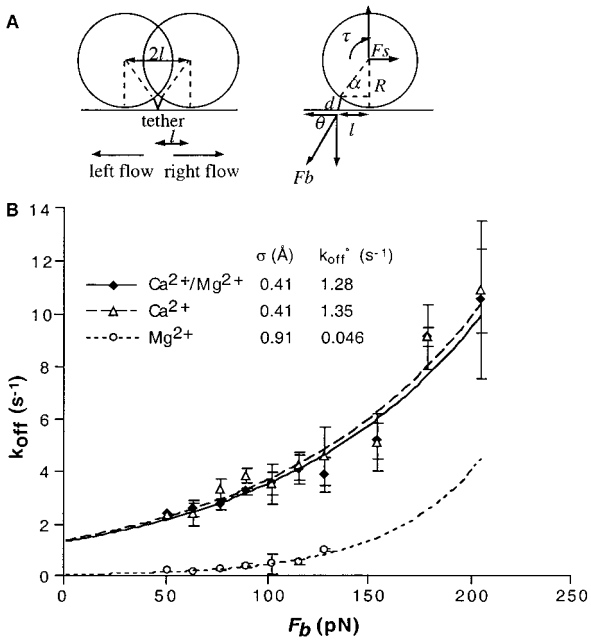

FIGURE 5: Relation of dissociation rate constant to force on the tether bond for $\alpha4\beta7$−MAdCAM-1 in the presence of different divalent cations. The k_{off} was measured at different wall shear stresses for RPMI 8866 cell transient tethers to MAdCAM-1. Data were collected in 1 mM Ca^{2+} + 1 mM Mg^{2+} (Ca^{2+}/Mg^{2+}), 1 mM Ca^{2+} (Ca^{2+}), or either 1 mM Mg^{2+} or 1.5 mM Mg^{2+} + 0.5 mM EGTA (Mg^{2+}). Data were collected at substrate densities of 15, 37.5, and 50 sites/μm^2 at 0.4−1 dyn/cm^2 and 37.5, 50, and 125 sites/μm^2 at 1.2−1.6 dyn/cm^2. At least 30 transient tethers were collected per data set. The number of data sets at each wall shear stress was 3−6, mean = 4.1 in Ca^{2+}/Mg^{2+}; 2−6, mean = 3.9 in Ca^{2+}; and 1−4, mean = 2.7 in Mg^{2+}. Error bars show SD. The data were fit to the Bell equation, $k_{off} = k_{off}^{\circ} \exp(\sigma F_b/kT)$ (lines). Inset: l, the lever arm, and the cell diameter were measured as described in the text. The Goldman equation was used to calculate the hydrodynamic torque, τ, and force on the cell, F_s. The force and torque balances on a tethered cell in shear flow are $F_b \cos\theta = F_s$ and $F_b l \sin\theta = \tau_s + RF_s$. Calculation yielded $d = 1.88 \pm 0.48$ μm, $\theta = 55.1 \pm 2.2°$, and $F_b/F_s = 1.74 \pm 0.1$ for RPMI 8866 cells on MAdCAM-1. The F_b at 1 dyn/cm^2 was 129 pN.

Comparison of k_{off} as a function of F_b revealed that the $\alpha4\beta7$−MAdCAM-1 tether bond is moderately force resistant (Figure 5). At wall shear stress giving F_b of 50 pN, the k_{off} was close to 2 s^{-1}. By contrast, at 210 pN the k_{off} increased moderately to 8 s^{-1}. As discussed in the introduction, several different exponential relationships between F_b and k_{off} have been proposed, and the best fit to experimental data has been found for the Bell model (*40*). In this model

$$k_{off} = k_{off}^{\circ} \exp(\sigma F_b/kT)$$

where k_{off}° is the unstressed k_{off}, σ is the bond interaction distance or mechanical bond length (the separation distance required to weaken the bond), k is Boltzmann's constant, and T is the absolute temperature (*37*). The Bell equation fit the data well (line, Figure 5) and yielded the estimate of k_{off}° of 1.28 ± 0.13 s^{-1}. This k_{off}° is comparable to those for P-selectin and E-selectin and markedly slower than for L-selectin (*3*, *29*). The mechanical bond length (σ) estimate is 0.41 ± 0.03 Å for the $\alpha4\beta7$−MAdCAM-1 tether bond, which is at the upper range of measurements for selectins.

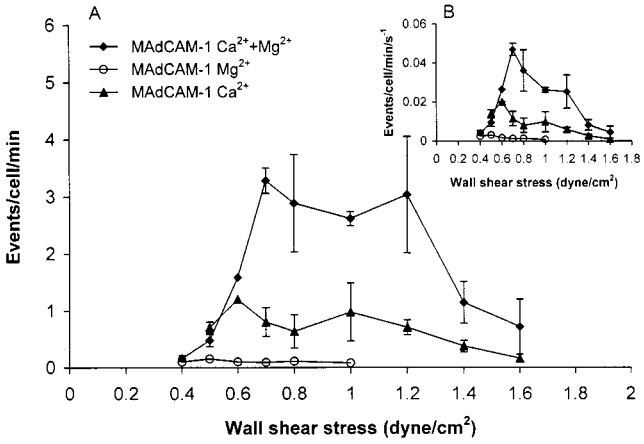

FIGURE 6: Frequency of transient tethers on MAdCAM-1 as a function of wall shear stress and divalent cations. The number of transient tethers per minute of RPMI 8866 cells on MAdCAM-1 was measured. (A) The number of transient tethers was divided by the number of cells on average in the focal plane in the field of view and by the number of minutes the data were collected. (B) Same data as in (A) but additionally divided by the shear rate to eliminate any effect of transport on the rate of bond formation. Divalent cations were as described in Figure 5.

To understand the contrasting effects of divalent cations on α4β7 integrin adhesive interactions in shear flow, transient tether kinetics were measured in Ca^{2+} or Mg^{2+} alone. The kinetics of tether dissociation in Ca^{2+} alone were indistinguishable from those in Ca^{2+} + Mg^{2+} (Figure 5). However, markedly differing effects were observed in Mg^{2+}. The $k_{off}°$ was much lower, 0.046 s^{-1} (Figure 5). This correlated well with the observation of rolling adhesion in Ca^{2+} plus Mg^{2+}, or Ca^{2+} alone, and firm adhesion in Mg^{2+} alone. The mechanical strength of the α4β7−MAdCAM-1 bond in Mg^{2+} was weaker, with a mechanical bond length of 0.91 Å.

Shear-Enhanced Adhesion through α4β7 and MAdCAM-1. Rolling is a function not only of the rate of bond dissociation but also of the rate of bond formation. Therefore, we examined the rate of formation of transient tethers as a function of wall shear stress and divalent cations. For MAdCAM-1 in Ca^{2+} and Mg^{2+}, tethering frequency increased markedly from 0.4 to 0.7 dyn/cm^2 (Figure 6A). Transport of the cell relative to the substrate, as well as diffusion of ligand binding domains, enhances receptor−ligand encounter and hence binding. The maximal amount of enhancement by transport is equal to the increase in velocity of cells relative to the substrate, which is proportional to the shear rate (*55*). To account for this, the rate of transient tethering was divided by the shear rate (Figure 6B). A very marked increase in the rate of tethering was seen as shear was increased between 0.4 and 0.7 dyn/cm^2, showing that factors other than transport are responsible for the enhancement by shear of the rate of bond formation. This has previously been seen for selectins and stabilizes rolling by compensating for increased k_{off} at higher shear (*28*, *29*). Above 0.7 dyn/cm^2 in Ca^{2+} and Mg^{2+}, the rate of transient tether formation decreased with higher shear. This can be explained by diminished time for bond formation after receptor−ligand encounter. Comparisons among cations for tethering efficiency revealed that tethering in Ca^{2+} alone was less efficient than in Ca^{2+} + Mg^{2+} but had a similar shear dependence (Figure 6). Tethering occurred in Mg^{2+} alone but was much less efficient.

DISCUSSION

Novel Requirement for Ca^{2+} for Rolling through α4 Integrins. We have made the novel finding that rolling through α4 integrins on MAdCAM-1 and VCAM-1 is dependent on the presence of Ca^{2+}. In contrast, firm adhesion of α4β7 to MAdCAM-1 is dependent on Mg^{2+}. Previous results in static binding assays have shown that both Ca^{2+} and Mg^{2+} support binding through α4β1 to VCAM-1 (*56*) and binding through α4β7 to MAdCAM-1 (*26*). Our findings are in agreement with these previous studies; however, the use of flow assays reveals that the adhesive modalities differ in Ca^{2+} and Mg^{2+}. We find that Ca^{2+} is very important for the initial tethering events mediated by α4 integrins, and in agreement with this, robust rolling through α4 integrins is observed on both MAdCAM-1 and VCAM-1 with Ca^{2+} as the only divalent cation.

The differing adhesive behaviors in Ca^{2+} and Mg^{2+} of α4β7 on MAdCAM-1 could be readily understood in terms of the kinetic constants measured for transient tethers. The $k_{off}°$ of the α4β7−MAdCAM-1 interaction was dramatically influenced by divalent cations; the $k_{off}°$ was 20-fold slower in Mg^{2+} compared to Ca^{2+}, favoring firm adhesion. As a surrogate for k_{on}, we measured the frequency of transient tethers. At a given shear, k_{on} should be proportional to transient tether frequency. This estimates the α4β7−MAdCAM-1 k_{on} in Mg^{2+} as at least 10-fold less than in Ca^{2+}. Again, the slower on-rate would disfavor rolling adhesion but would be conducive for the firm adhesion seen in Mg^{2+}. To summarize these results, the α4β7−MAdCAM-1 tether has both a faster k_{on} and $k_{off}°$ in Ca^{2+} than in Mg^{2+}, resulting in rolling in Ca^{2+} and firm adhesion in Mg^{2+}.

The relationship of putative Ca^{2+} and Mg^{2+} binding sites in integrins to the distinct Ca^{2+}-dependent and Mg^{2+}-dependent adhesive modalities of α4 integrins will be interesting to determine. We found that Ca^{2+} supports rolling through both α4 integrins, whereas Mg^{2+} cannot support rolling but can support firm adhesion through α4β7. A different type of distinction between Ca^{2+} and Mg^{2+} was previously found in static adhesion assays; both Ca^{2+} and Mg^{2+} support α4β1 adhesion to VCAM-1, but Mg^{2+} supports binding to fibronectin much better than Ca^{2+} (*56*). To mediate these effects, Ca^{2+} and Mg^{2+} might be present in common or distinct ligand binding sites, or Ca^{2+} and Mg^{2+} might bind elsewhere and allosterically regulate ligand binding. Using mAb to different α4 epitopes (*57*), we have not been able to obtain evidence for topographically distinct ligand binding sites in Ca^{2+} and Mg^{2+}. The α4 mAbs to the B1 and B2 epitopes inhibit both rolling and firm adhesion through α4β7, whereas mAb to the A and C epitopes inhibit neither (data not shown). It is doubtful that the putative Ca^{2+} binding sites on the bottom of the β-propeller domain (*58*, *59*) are directly involved in ligand binding, because ligand binding loops map to the upper face of the β-propeller (*60*). Furthermore, mutations of the Ca^{2+} binding loops that do not disrupt structure do not affect tethering in shear flow, but do affect adhesion strengthening (*61*). This is the opposite of what would be expected if these loops were involved in the Ca^{2+}-dependent rolling adhesive modality. In the integrin αMβ2, binding of an antibody to a Ca^{2+} binding loop is supported equally well by Ca^{2+} and Sr^{2+} (*62*), whereas we showed here that Ca^{2+} but not Sr^{2+} supports tethering in shear flow. Thus,

the β-hairpin loop Ca^{2+} binding motifs on the bottom of the β-propeller do not appear to represent a Ca^{2+}-dependent binding site or an allosteric site responsible for Ca^{2+}-dependent regulation of rolling. Interestingly, Ca^{2+} has recently been found to bind to the β-subunit I-like domain and possibly to its MIDAS motif (*63*). An attractive possibility is that Mg^{2+} and Ca^{2+} might compete for this site and favor firm adhesion and rolling adhesion, respectively. However, caution is required in interpreting results with respect to currently known metal binding sites, because further Ca^{2+} and Mg^{2+} binding sites may be revealed by integrin structures. Further work will be required to define the specific metal binding sites that regulate the α4 integrin rolling and firm adhesion modalities.

Rolling though α4 Integrins Compared to Selectins. Compared to selectins, we found that rolling through the α4 integrins was less stable; it was more prone to develop into detachment or firm adhesion. Furthermore, the range of site densities yielding optimal rolling through α4 integrins was limited, with firm adhesion seen on MAdCAM-1 above 150 sites/μm^2 and on VCAM-1 above 100 sites/μm^2. By contrast, neutrophils can roll on E-selectin over a range of 35−900 sites/μm^2 (*52*).

Recent studies have shown that several types of molecular specializations are required to support rolling (*3*, *28*, *33*). Rolling as an adhesive state is delicately poised between firm adhesion and detachment. For rolling to be maintained, the rate of formation of new bonds must be balanced by the rate of bond dissociation. Otherwise, for example, a decrease in wall shear stress and hence in rate of bond breakage would lead to firm adhesion. Few adhesion molecules or antibodies to cell surface molecules can support rolling, and rolling on the small subset of antibodies that can support rolling is unstable and occurs over only a narrow window of wall shear stresses and substrate densities (*33*). By contrast, on P-selectin, E-selectin, and L-selectin, firm adhesion is never seen. This is because of an "automatic braking system", in which increase in wall shear increases the rate of formation of new bonds and therefore compensates for the increase in rate of bond breakage (*28*). Shear-enhanced bond formation during rolling by selectins is mirrored by shear-enhanced formation of transient tethers through selectins (*28, 29*). Here, shear-enhanced tether formation was seen for α4β7−MAdCAM-1 (Figure 6) but not α4β1−VCAM-1 (data not shown). Although transport can enhance bond formation (*29*, *55*), this made only a small contribution to the amount of enhancement observed. It will be interesting to determine whether shear enhancement of bond formation is related to any molecular characteristic, such as the shared presence of mucin-like domains in MAdCAM-1 and selectin ligands but not in VCAM-1.

Rapid rates of bond formation and breakage are required for rolling; k_{off}° values determined for the α4β7−MAdCAM-1 receptor−ligand bond in the presence of Ca^{2+} and in the presence of Ca^{2+} and Mg^{2+} were within the range previously found for selectins (Table 1). By contrast, the k_{off}° of 0.046 s^{-1} for the interaction in Mg^{2+} of α4β7 with MAdCAM-1 was not within this range. Notably, this interaction did not support rolling and did support firm adhesion.

A mechanically stable bond stabilizes rolling by moderating the amount by which force increases k_{off}. The exponential constant σ, which represents the bond interaction distance, was used as an estimate of mechanical bond strength. The higher the σ, the weaker the bond. The σ for the α4β7−MAdCAM-1 tether bond in Ca^{2+} and in $Ca^{2+} + Mg^{2+}$ was moderately to slightly higher than σ values found for L-selectin, E-selectin, and P-selectin (Table 1). This is consistent with the ability of the α4β7−MAdCAM-1 receptor ligand bond to support rolling. By contrast, the α4β7−MAdCAM-1 bond in the presence of Mg^{2+} is markedly mechanically weaker and did not support rolling.

Table 1: Kinetic and Mechanical Properties of Cell−Substrate Tether Bonds

cell surface	substrate	k_{off}° (s^{-1})	σ (Å)	ref[a]
L-selectin	PNAd	6.80	0.20	*29*
L-selectin	PNAd	8.60	0.16	*34*
ligand	L-selectin	7.00	0.24	*32*
ligand	E-selectin	0.70	0.31	*29*
PSGL-1	P-selectin	0.93	0.40	*3, 29*
PSGL-1	P-selectin	1.10	0.29	*34*
α4β7/CaMg	MAdCAM-1	1.28	0.41	this paper
α4β7/Ca	MAdCAM-1	1.35	0.41	this paper
α4β7/Mg	MAdCAM-1	0.046	0.91	this paper
CD15	mAb PM-81	2.05	0.88	*33*

[a] Kinetic and mechanical properties were also measured for selectins by Smith et al. (*35*), but points at higher forces were omitted in the curve fits used to estimate k_{off}° and σ.

Our findings demonstrate two different adhesive modalities for α4 integrins, one in Ca^{2+} and one in Mg^{2+}, both of which appear to operate under physiological conditions in which both Ca^{2+} and Mg^{2+} are present. These findings explain the heretofore surprising observations that α4 integrins can mediate both rolling adhesion and firm adhesion. Furthermore, our studies on the kinetic and mechanical properties of the α4β7 interaction with MAdCAM-1 suggest that it is well suited for the intermediate position that α4 integrins occupy in the leukocyte-endothelial adhesive cascade in the vasculature. In the adhesive cascade in Peyer's patch, α4β7 integrins function downstream of L-selectin and upstream of αLβ2 (*43*). Interactions that are more upstream should have faster k_{off} than those downstream. Appropriately, the k_{off}° of L-selectin is faster than that of α4β7 (Table 1). E-selectin and P-selectin are also downstream of L-selectin leukocyte−leukocyte interactions in adhesive cascades (*54*) and appropriately have k_{off}° values similar to those of α4β7 (Table 1). Mechanically stable bonds are most important early in adhesive cascades, because more receptor−ligand bonds accumulate later in the cascade, and the hydrodynamic force experienced by the cell is distributed over a larger number of bonds, and hence is lower per bond. The α4β7−MAdCAM-1 bond is slightly less mechanically stable than any selectin bond (Table 1). These findings are appropriate for the function of α4 integrins in intermediate positions in adhesion cascades, downstream of selectins and upstream of β2 integrins (*41*−*43*, *54*).

NOTE ADDED IN PROOF

An integrin crystal structure confirms that Ca^{2+} binds to integrin I-like domains as discussed above and demonstrates that Mg^{2+} and Ca^{2+} binding sites are adjacent in the ligand binding site (*64*).

REFERENCES

1. Butcher, E. C. (1991) *Cell 67*, 1033−1036.
2. Springer, T. A. (1994) *Cell 76*, 301−314.
3. Alon, R., Hammer, D. A., and Springer, T. A. (1995) *Nature 374*, 539.
4. Berlin, C., Bargatze, R. F., von Andrian, U. H., Szabo, M. C., Hasslen, S. R., Nelson, R. D., Berg, E. L., Erlandsen, S. L., and Butcher, E. C. (1995) *Cell 80*, 413−422.
5. Tözeren, A., Kleinman, H. K., Wu, S., Mercurio, A. M., and Byers, S. W. (1994) *J. Cell Sci. 107*, 3153−3163.
6. Knorr, R., and Dustin, M. L. (1997) *J. Exp. Med. 186*, 719−730.
7. Sigal, A., Bleijs, D. A., Grabovsky, V., van Vliet, S. J., Dwir, O., Figdor, C. G., van Kooyk, Y., and Alon, R. (2000) *J. Immunol. 165*, 442−452.
8. Elices, M. J., Osborn, L., Takada, Y., Crouse, C., Luhowskyj, S., Hemler, M. E., and Lobb, R. R. (1990) *Cell 60*, 577−584.
9. Briskin, M. J., McEvoy, L. M., and Butcher, E. C. (1993) *Nature 363*, 461−464.
10. Osborn, L., Hession, C., Tizard, R., Vassallo, C., Luhowskyj, S., Chi-Rosso, G., and Lobb, R. (1989) *Cell 59*, 1203−1211.
11. Streeter, P. R., Lakey-Berg, E., Rouse, B. T. N., Bargatze, R. F., and Butcher, E. C. (1988) *Nature 331*, 41−46.
12. Berg, E. L., McEvoy, L. M., Berlin, C., Bargatze, R. F., and Butcher, E. C. (1993) *Nature 366*, 695−698.
13. Hynes, R. O. (1992) *Cell 69*, 11−25.
14. Luque, A., Sanchez-Madrid, F., and Cabanas, C. (1994) *FEBS Lett. 346*, 278−284.
15. Staatz, W. D., Rajpara, S. M., Wayner, E. A., Carter, W. G., and Santoro, S. A. (1989) *J. Cell Biol. 108*, 1917−1924.
16. Kern, A., Eble, J., Golbik, R., and Kuhn, K. (1993) *Eur. J. Biochem. 215*, 151−159.
17. Weitzman, J. B., Wells, C. E., Wright, A. H., Clark, P. A., and Law, S. K. A. (1991) *FEBS Lett. 294*, 97−103.
18. Elices, M. J., Urry, L. A., and Hemler, M. E. (1991) *J. Cell Biol. 112*, 169−181.
19. Sonnenberg, A., Modderman, P. W., and Hogervorst, F. (1988) *Nature 336*, 487−489.
20. Kirchhofer, D., Grzesiak, J., and Pierschbacher, M. D. (1991) *J. Biol. Chem. 266*, 4471−4477.
21. Dransfield, I., Cabañas, C., Craig, A., and Hogg, N. (1992) *J. Cell Biol. 116*, 219−226.
22. Mould, A. P., Akiyama, S. K., and Humphries, M. J. (1995) *J. Biol. Chem. 270*, 26270−26277.
23. Grzesiak, J. J., Davis, G. E., Kirchhofer, D., and Pierschbacher, M. D. (1992) *J. Cell Biol. 117*, 1109−1117.
24. Smith, J. W., Piotrowicz, R. S., and Mathis, D. (1994) *J. Biol. Chem. 269*, 960−967.
25. Masumoto, A., and Hemler, M. E. (1993) *J. Cell Biol. 123*, 245−253.
26. Tidswell, M., Pachynski, R., Wu, S. W., Qiu, S.-Q., Dunham, E., Cochran, N., Briskin, M. J., Kilshaw, P. J., Lazarovits, A. I., Andrew, D. P., Butcher, E. C., Yednock, T. A., and Erle, D. J. (1997) *J. Immunol. 159*, 1497−1505.
27. Alon, R., Kassner, P. D., Carr, M. W., Finger, E. B., Hemler, M. E., and Springer, T. A. (1995) *J. Cell Biol. 128*, 1243−1253.
28. Chen, S., and Springer, T. A. (1999) *J. Cell Biol. 144*, 185−200.
29. Alon, R., Chen, S., Puri, K. D., Finger, E. B., and Springer, T. A. (1997) *J. Cell Biol. 138*, 1169−1180.
30. Lawrence, M. B., and Springer, T. A. (1991) *Cell 65*, 859−873.
31. Puri, K. D., Chen, S., and Springer, T. A. (1998) *Nature 392*, 930−933.
32. Alon, R., Chen, S., Fuhlbrigge, R., Puri, K. D., and Springer, T. A. (1998) *Proc. Natl. Acad. Sci. U.S.A. 95*, 11631−11636.
33. Chen, S., Alon, R., Fuhlbrigge, R. C., and Springer, T. A. (1997) *Proc. Natl. Acad. Sci. U.S.A. 94*, 3172−3177.
34. Ramachandran, V., Nollert, M. U., Qiu, H., Liu, W. J., Cummings, R. D., Zhu, C., and McEver, R. P. (1999) *Proc. Natl. Acad. Sci. U.S.A. 96*, 13771−13776.
35. Smith, M. J., Berg, E. L., and Lawrence, M. B. (1999) *Biophys. J. 77*, 3371−3383.
36. Zhurkov, S. N. (1966) *Int. J. Fract. Mech. 1*, 311−323.
37. Bell, G. I. (1978) *Science 200*, 618−627.
38. Evans, E., and Ritchie, K. (1997) *Biophys. J. 72*, 1541−1555.
39. Dembo, M., Torney, D. C., Saxman, K., and Hammer, D. (1988) *Proc. R. Soc. London, Ser. B 234*, 55−83.
40. Chen, S., and Springer, T. A. (2001) *Proc. Natl. Acad. Sci. U.S.A. 98*, 950−955.
41. Luscinskas, F. W., Kansas, G. S., Ding, H., Pizcueta, P., Schleiffenbaum, B. E., Tedder, T. F., and Gimbrone, M. A., Jr. (1994) *J. Cell Biol. 125*, 1417−1427.
42. Jones, D. A., McIntire, L. V., Smith, C. W., and Picker, L. J. (1994) *J. Clin. Invest. 94*, 2443−2450.
43. Bargatze, R. F., Jutila, M. A., and Butcher, E. C. (1995) *Immunity 3*, 99−108.
44. Johnston, B., Walter, U. M., Issekutz, A. C., Issekutz, T. B., Anderson, D. C., and Kubes, P. (1997) *J. Immunol. 159*, 4514−4523.
45. Stupack, D. G., Stewart, S., Carter, W. G., Wayner, E. A., and Wilkins, J. A. (1991) *Scand. J. Immunol. 34*, 761−769.
46. Kassner, P. D., and Hemler, M. E. (1993) *J. Exp. Med. 178*, 649−660.
47. Lu, C., and Springer, T. A. (1997) *J. Immunol. 159*, 268−278.
48. Briskin, M., Winsor-Hines, D., Shyjan, A., Cochran, N., Bloom, S., Wilson, J., McEvoy, L. M., Butcher, E. C., Kassam, N., Mackay, C. R., Newman, W., and Ringler, D. J. (1997) *Am. J. Pathol. 151*, 97−110.
49. Lobb, R. R., Chi-Rosso, G., Leone, D. R., Rosa, M. D., Bixler, S., Newman, B. M., Luhowskyj, S., Benjamin, C. D., Dougas, I. R., Goelz, S. E., Hession, C., and Chow, E. P. (1991) *J. Immunol. 147*, 124−129.
50. Springer, T. A., Luther, E., and Klickstein, L. B. (1995) in *Leukocyte typing V: White cell differentiation antigens* (Schlossman, S. F., Boumsell, L., Gilks, W., Harlan, J., Kishimoto, T., Morimoto, T., Ritz, J., Shaw, S., Silverstein, R., Springer, T., Tedder, T., and Todd, R., Eds.) pp 1443−1467, Oxford University Press, New York.
51. Lu, C., Oxvig, C., and Springer, T. A. (1998) *J. Biol. Chem. 273*, 15138−15147.
52. Lawrence, M. B., and Springer, T. A. (1993) *J. Immunol. 151*, 6338−6346.
53. Vonderheide, R. H., Tedder, T. F., Springer, T. A., and Staunton, D. E. (1994) *J. Cell Biol. 125*, 215−222.
54. Alon, R., Fuhlbrigge, R. C., Finger, E. B., and Springer, T. A. (1996) *J. Cell Biol. 135*, 849−865.
55. Chang, K. C., and Hammer, D. A. (1999) *Biophys. J. 76*, 1280−1292.
56. Masumoto, A., and Hemler, M. E. (1993) *J. Biol. Chem. 268*, 228−234.
57. Pulido, R., Elices, M. J., Campanero, M. R., Osborn, L., Schiffer, S., García-Pardo, A., Lobb, R., Hemler, M. E., and Sánchez-Madrid, F. (1991) *J. Biol. Chem. 266*, 10241−10245.
58. Springer, T. A. (1997) *Proc. Natl. Acad. Sci. U.S.A. 94*, 65−72.
59. Springer, T. A., Jing, H., and Takagi, J. (2000) *Cell 102*, 275−277.
60. Irie, A., Kamata, T., and Takada, Y. (1997) *Proc. Natl. Acad. Sci. U.S.A. 94*, 7198−7203.
61. Pujades, C., Yauch, R., Alon, R., Masumoto, A., Burkly, L., Springer, T. A., Chen, C., Lobb, R. R., and Hemler, M. E. (1997) *Mol. Biol. Cell 8*, 2647−2657.
62. Oxvig, C., and Springer, T. A. (1998) *Proc. Natl. Acad. Sci. U.S.A. 95*, 4870−4875.
63. Xiong, Y., and Zhang, L. (2001) *J. Biol. Chem. 276*, 19340−19349.
64. Xiong, J.-P., Stehle, T., Diefenbach, B., Zhang, R., Dunker, R., Scott, D. L., Joachimiak, A., Goodman, S. L., and Arnaout, M. A. (2001) *Science 294*, 339−345.

BI011582F